nature immunology

Epithelial microRNAs regulate gut mucosal immunity via epithelium–T cell crosstalk

Moshe Biton[1,9], Avi Levin[1,2,9], Michal Slyper[1], Irit Alkalay[1], Elad Horwitz[1], Hagar Mor[1], Sharon Kredo-Russo[3], Tali Avnit-Sagi[4], Gady Cojocaru[1], Farid Zreik[5], Zvi Bentwich[6], Matthew N Poy[7], David Artis[8], Michael D Walker[4], Eran Hornstein[3], Eli Pikarsky[1,5] & Yinon Ben-Neriah[1]

Colonic homeostasis entails epithelium-lymphocyte cooperation, yet many participants in this process are unknown. We show here that epithelial microRNAs mediate the mucosa–immune system crosstalk necessary for mounting protective T helper type 2 (T_H2) responses. Abolishing the induction of microRNA by gut-specific deletion of *Dicer1* (*Dicer1*$^{\Delta gut}$), which encodes an enzyme involved in microRNA biogenesis, deprived goblet cells of RELMβ, a key T_H2 antiparasitic cytokine; this predisposed the host to parasite infection. Infection of *Dicer1*$^{\Delta gut}$ mice with helminths favored a futile T_H1 response with hallmarks of inflammatory bowel disease. Interleukin 13 (IL-13) induced the microRNA miR-375, which regulates the expression of TSLP, a T_H2-facilitating epithelial cytokine; this indicated a T_H2-amplification loop. We found that miR-375 was required for RELMβ expression *in vivo*; miR-375-deficient mice had significantly less intestinal RELMβ, which possibly explains the greater susceptibility of *Dicer1*$^{\Delta gut}$ mice to parasites. Our findings indicate that epithelial microRNAs are key regulators of gut homeostasis and mucosal immunity.

The colon epithelium is a busy arena for innate immunity. A single layer of epithelial cells forms a barrier that separates the host from luminal microflora. Unexpectedly, this abundant microflora does not elicit overt inflammation in the intestinal mucosa under normal physiological conditions. Whereas many of the microflora-tolerance mechanisms are yet to be identified, studies have indicated the involvement of intestinal epithelial cell (IEC) factors in this tolerance. Among these are factors that control the central inflammatory mediator NF-κB, components of the IEC physical barrier and their polarized configuration, specialized mucus secretion by goblet cells and more[1–4]. Disruption of any of the factors described above impairs gut tolerance to microflora and leads to sustained immune activation that often results in the chronic inflammation that possibly leads to inflammatory bowel disease[3,5].

MicroRNAs (miRNAs) have emerged as important regulators of many biological processes[6,7]. Hundreds of miRNAs, many evolutionarily conserved, have been identified in mammals, but their physiological functions are just beginning to be elucidated[8]. Although it seems that the expression of some miRNAs is ubiquitous, the expression of most is tightly regulated in a temporal and tissue-specific manner[9]. Accumulating data indicate that miRNAs are part of the complex regulatory networks that control various cells types, such as the fate of epithelial cells and cells of the immune system, during mammalian development and adult tissue renewal[10,11]. Two main enzymes involved in miRNA biogenesis are Dicer and Drosha, and conditional deletion of the gene encoding either of these is sufficient to abolish the pathway of RNA-mediated interference and microRNA and is useful as a means of studying the role of miRNAs in the physiology of a specific tissue[10–13].

To address the role of IEC miRNAs in gut homeostasis, we inactivated *Dicer1* specifically in the IECs of adult mice. The main outcome was fewer goblet cells and a lower abundance of the goblet cell–specific T_H2 effector RELMβ in the colon, accompanied by immunological defects that compromised parasite resistance. By combining *in vivo* and *in vitro* approaches, we have identified an epithelium-expressed miRNA, miR-375, as a key regulator of epithelial properties that are necessary for securing epithelium–immune system crosstalk. This mucosal circuit propagates a T_H2 amplification loop, which is needed to maintain gut immunity and homeostasis.

RESULTS

Deleting *Dicer1* in the gut leads to goblet-cell depletion

Mucus-secreting goblet cells make up about 80% of the colon epithelium[14]. After inducible gut-specific deletion of *Dicer1* (*Dicer1*$^{\Delta gut}$), we observed ~90% lower *Dicer1* expression (**Supplementary Fig. 1**) concomitant with fewer mature goblet cells (**Fig. 1**). The depletion

[1]Lautenberg Center for Immunology, Hebrew University-Hadassah Medical School, Jerusalem, Israel. [2]Department of Gastroenterology, Division of Medicine, Hebrew University-Hadassah Medical Center, Jerusalem, Israel. [3]Department of Molecular Genetics, Weizmann Institute of Science, Rehovot, Israel. [4]Department of Biological Chemistry, Weizmann Institute of Science, Rehovot, Israel. [5]Department of Pathology, Hebrew University Hadassah Medical School, Jerusalem, Israel. [6]Rosetta Genomics, Rehovot, Israel. [7]Max-Delbrück-Center for Molecular Medicine, Berlin, Germany. [8]Department of Microbiology and Institute for Immunology, School of Medicine, and Department of Pathobiology, School of Veterinary Medicine, University of Pennsylvania, Philadelphia, Pennsylvania, USA. [9]These authors contributed equally to this work. Correspondence should be addressed to E.P. (peli@hadassah.org.il) or Y.B.-N. (yinon@cc.huji.ac.il).

Received 6 December 2010; accepted 10 January 2011; published online 30 January 2011; doi:10.1038/ni.1994

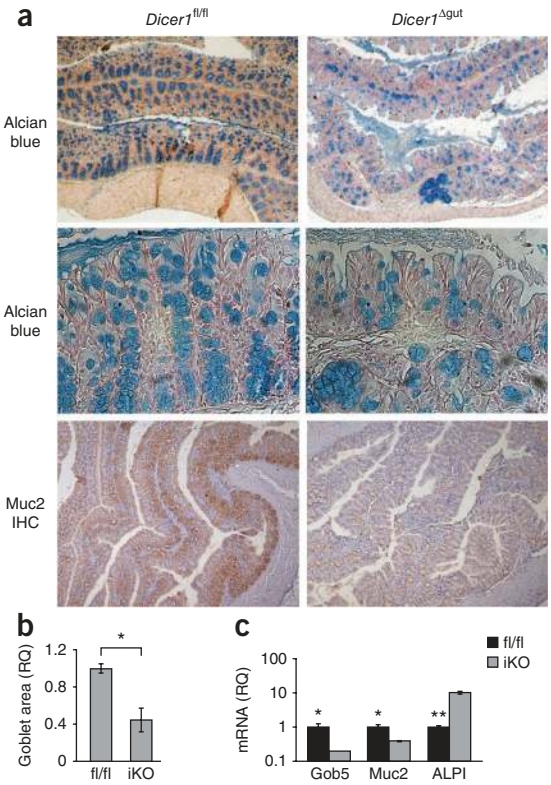

Figure 1 Inducible ablation of *Dicer1* specifically in the gut epithelium results in depletion of goblet cells. (**a**) Formalin-fixed, paraffin-embedded (FFPE) colon sections from *Dicer1*$^{fl/fl}$ mice and *Dicer1*$^{\Delta gut}$ mice (1 month after induction), stained with Alcian blue (which stains mature goblet cells; top and middle), and immunohistochemistry of Muc2 (bottom). Original magnification, ×50 (top and bottom) or ×200 (middle). (**b**) Goblet-cell quantification by automated image analysis of colon sections from *Dicer1*$^{fl/fl}$ mice (fl/fl) and *Dicer1*$^{\Delta gut}$ mice (iKO), calculated as the ratio of the Alcian blue–positive area to the nuclear area and presented as relative quantification (RQ) relative to the value for *Dicer1*$^{fl/fl}$ mice, set as 1. $*P = 0.003$ (*t*-test). (**c**) Quantitative PCR analysis of the goblet cell markers Gob5 and Muc2 and the enterocyte marker alkaline phosphatase (ALPI) in colon epithelial cells from *Dicer1*$^{fl/fl}$ and *Dicer1*$^{\Delta gut}$ littermates, presented (in logarithmic scale) relative to the expression in *Dicer1*$^{fl/fl}$ cells, set as 1. $*P = 0.05$ and $**P = 0.003$ (*t*-test). Data are representative of three experiments (**a**), one experiment (**b**; mean ± s.e.m. of three mice per group) or two experiments (**c**; mean ± s.e.m. of three mice per group).

of goblet cells was evident by staining of the mucus with Alcian blue and by immunohistochemistry for Mucin2 (Muc2), a goblet cell–specific marker (**Fig. 1a**). Automated quantitative image analysis indicated that the area stained by Alcian blue was ~50% smaller in *Dicer1*$^{\Delta gut}$ mice than in control mice with *lox*P-flanked *Dicer1* (*Dicer1*$^{fl/fl}$; **Fig. 1b**). In addition, we noted lower expression of mRNA for the goblet cell–specific markers Muc2 and Gob5 (a chloride channel accessory protein) and higher expression of mRNA for the enterocyte-specific marker alkaline phosphatase[4,15] (**Fig. 1c**). Notably, we found neither more apoptosis nor proliferation defects in *Dicer1*$^{\Delta gut}$ colon epithelium (**Supplementary Fig. 2**), which suggested that goblet-cell differentiation, rather than cell death or proliferation, was affected by *Dicer1* ablation, presumably through deficient miRNA activity.

Regulation of goblet-cell differentiation by miR-375

To better understand the mechanism of goblet-cell depletion in the *Dicer1*$^{\Delta gut}$ colon, we did an *in vitro* differentiation assay of HT-29 cells, a colorectal cancer cell line that under certain conditions has the ability to differentiate into various gut epithelial cells, such as enterocytes and goblet cells[16] (**Supplementary Fig. 3a**). Sodium butyrate–treated HT-29 cells underwent dedifferentiation, after which they redifferentiated randomly into enterocytes or goblet cells[17]. We isolated specific cell clones by limiting dilution of differentiated cells (**Supplementary Fig. 3a**,**b**). Using specific intestine cell markers[15], we generated two clonal cultures: CF1, with goblet cell–like features, and CF2, which resembled enterocytes (**Supplementary Fig. 3b**,**c**).

To determine whether miRNAs are required for goblet-cell maturation, we depleted HT-29 cells of Drosha before differentiation[18] (**Supplementary Fig. 3d**). We preferred depletion of Drosha because, unlike depletion of Dicer, it can be followed by confirmatory experiments with reconstitution by precursor miRNAs[7]. Knockdown of Drosha abolished goblet-cell differentiation (**Fig. 2a**,**b**), reminiscent of the phenotype of *Dicer1*$^{\Delta gut}$ mice (**Fig. 1**). We therefore used this *in vitro* system to identify factors that mediate miRNA-dependent maturation of goblet cells.

To detect miRNAs that affect IEC differentiation, we assessed a set of miRNAs identified in colonic diseases (such as colon cancer and inflammatory bowel disease)[19–21]. Although the expression of most miRNAs did not differ much in the various HT-29 clones, we noted 'preferential' expression of miR-375 in the CF1 goblet clone. This clone (CF1) had tenfold higher miR-375 expression than did the enterocyte cell clone (CF2), whereas the expression of miR-107 and miR-200a was similar in the two cell clones (**Fig. 2c**). To determine whether miR-375 affects goblet-cell differentiation, we overexpressed miR-375 in HT-29 cells (**Supplementary Fig. 3e**). We then subjected HT29 cells overexpressing miR-375 to the *in vitro* differentiation assay. More extensive goblet-cell differentiation was induced by overexpression of miR-375 but not by overexpression of miR-16 (**Supplementary Fig. 3f**), which indicated that miR-375 is involved in goblet-cell differentiation. Next we tested whether miR-375 overexpression was sufficient to reconstitute goblet-cell differentiation in HT-29 cells depleted of Drosha. We found that miR-375 overexpression overcame the *Drosha*-silencing effect and resulted in enhanced Muc2 mRNA, resembling that of fully differentiated HT-29 cells (**Fig. 2d**). Thus, miR-375 expression 'rescued' the *Drosha*-silencing effect in the absence of any other miRNA and enabled goblet-cell differentiation *in vitro*. To assess the expression pattern of miR-375 in the gut, we analyzed transgenic reporter mice with expression of enhanced green fluorescent protein driven by the miR-375 promoter (768 base pairs)[22] and found activity of the miR-375 promoter selectively in epithelial cells with goblet-cell features in the colon and the small bowel (**Fig. 2e** and **Supplementary Fig. 3g**). Next we did laser-capture microdissection of the colonic 'stroma' and mucosa of wild-type C57BL/6 mice; this confirmed the mucosal specificity of miR-375 expression (**Fig. 2f** and **Supplementary Fig. 3h**). Finally, the absence of detectable miR-375 in mesenteric lymph nodes (data not shown) contradicted the possibility that miR-375 is expressed in mucosal lymphocytes.

A mouse strain with germline constitutive deficiency in miR-375 has been derived and found to have altered pancreatic beta-cell differentiation[23]. We analyzed these mice for goblet-cell markers and found they had less Gob5 mRNA than their control littermates had (**Fig. 2g**). Unlike results obtained with *Dicer1*$^{\Delta gut}$ mice, we did not detect a substantial change in goblet-cell numbers in the miR-375-deficient mice, as measured by Alcian blue staining (data not shown), yet the lower *in vivo* expression of Gob5, as

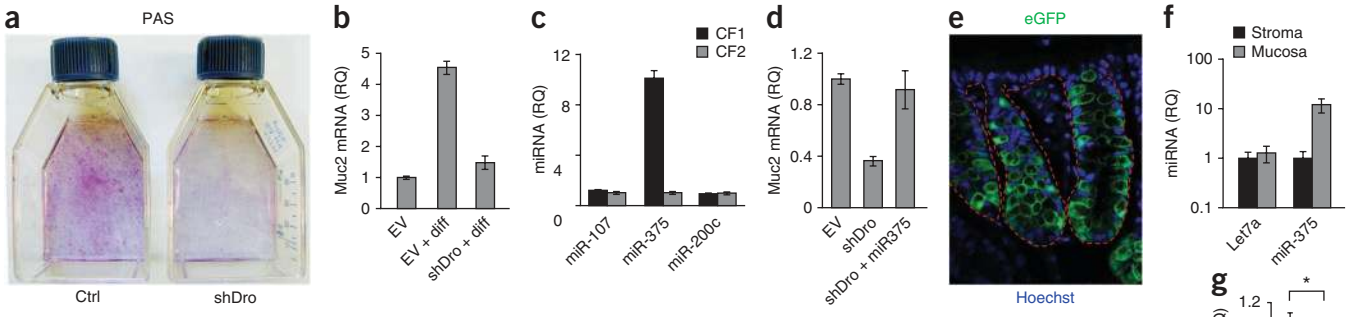

Figure 2 The microRNA miR-375 is a key factor in goblet cell differentiation. (**a**) Periodic acid–Schiff (PAS) staining of HT-29 cells in which *Drosha* was silenced (shDro) and control HT-29 cells treated with empty vector (Ctrl); red staining indicates mucus-secreting goblet cells. (**b**) Muc2 mRNA in undifferentiated HT-29 cells treated with empty vector (EV), differentiated HT-29 cells treated with empty vector (EV + diff) and differentiated HT-29 cells in which *Drosha* was silenced (shDro + diff); results are presented relative to the expression in undifferentiated cells treated with empty vector, set as 1. (**c**) Expression of miR-200c, miR-107 and miR-375 in clones CF1 (goblet cell) and CF2 (enterocyte), presented relative to expression in CF2, set as 1. (**d**) Expression of Muc2 mRNA in fully differentiated HT-29 cells treated with empty vector and in HT-29 cells in which *Drosha* was silenced with (shDro + miR375) or without (shDro) overexpression of miR-375; results are presented relative to the expression in cells treated with empty vector, set as 1. (**e**) Immunofluorescence analysis of colonic cryosections of mice transgenic for expression of enhanced green fluorescent protein (eGFP) via the miR-375 promoter, counterstained with Hoechst stain. The dashed line demarcates the border between the epithelium and the lamina propria. Original magnification, ×400. (**f**) Quantitative PCR analysis of the miRNA Let7a and miR-375 in colonic 'stroma' and mucosa isolated from FFPE sections by laser-capture microdissection, presented (in logarithmic scale) relative to the expression in 'stroma', set as 1. (**g**) Quantitative PCR analysis of Gob5 mRNA in whole-colon tissue from miR-375-deficient mice (miR-375-KO) and their wild-type littermates (WT), presented relative to the expression in wild-type mice, set as 1. $*P = 0.04$ (*t*-test). Data are representative of two independent experiments (**a**–**c**; mean ± s.e.m. in **b**,**c**), one experiment (**d**,**f**; mean ± s.e.m. in **d** and mean ± s.e.m. of ten fields per group in **f**) or two experiments (**e**,**g**; mean ± s.e.m. of five mice per group in **g**).

well as of RELMβ, another important goblet cell effector (discussed below), indicated a goblet cell–differentiation deficit attributable to miR-375 deletion.

Targeting of the goblet-cell regulator KLF5 by miR-375

Goblet-cell differentiation is mediated by several transcription factors, including KLF4 and Math1 (ref. 24). To understand the miRNA–goblet-cell connection, we scanned for predicted target genes of miR-375 with the TargetScan 5 program[25]. Among the various genes that could influence goblet-cell differentiation, we found that the 3′ untranslated regions (3′ UTRs) of mRNA encoding KLF4 and its antagonist KLF5 had a high miR-375 context score percentiles of 62 and 81, respectively (**Supplementary Fig. 4a**). The KLF family of zinc-finger transcription factors regulates a range of biological processes, including cell growth, differentiation, embryogenesis and tumorigenesis[26]. KLF5 antagonizes the activity of KLF4, a transcription factor essential for goblet-cell differentiation[26,27]. We therefore hypothesized that the downregulation of KLF5 by miR-375 in goblet-cell progenitors promotes their differentiation.

To address our hypothesis, we first measured KLF5 in the *Dicer1*-knockout model. KLF5 protein expression in wild-type mice was restricted to the lower part of the crypts, where it enabled the proliferation of and suppressed the differentiation of the progenitor cells located there (**Fig. 3a**). At 1 week after *Dicer1* ablation, KLF5 expression extended over most of the crypt length, and by 1 month after ablation, the entire crypt was $KLF5^+$ (**Fig. 3a**). Automated quantitative image analysis confirmed the time-dependent increase in KLF5 expression after *Dicer1* ablation throughout the entire colon crypt: there was tenfold more KLF5 staining in the epithelium top segments of the $Dicer1^{\Delta gut}$ colon crypts by 1 month after ablation (**Fig. 3b**). These findings raised the hypothesis that ectopic KLF5 expression accounted for the lack of goblet-cell maturation in the $Dicer1^{\Delta gut}$ colon. As $Dicer1^{\Delta gut}$ mice did not have more KLF5 mRNA (**Supplementary Fig. 4b**), we assume that KLF5 regulation is translational or post-translational.

To determine whether miR-375 controls the amount of KLF5 protein, we studied the regulation of KLF5 in HT-29 cells. After *Dicer* silencing, KLF5 mRNA was unchanged (**Supplementary Fig. 4c**), yet we noted more KLF5 protein in both clones (CF1 and CF2; **Fig. 3c**), which indicated miRNA-dependent inhibition of KLF5 translation. To determine whether KLF5 is directly regulated by miR-375, we inactivated this miRNA by transfecting HT-29 cells with an antisense oligonucleotide (antagomir) to miR-375. We observed KLF5 upregulation after knockdown of miR-375 but not when we used an antagomir with a scrambled sequence (**Fig. 3d**). To further verify that miR-375 specifically targets KLF5, we did a luciferase reporter assay of 3′ UTRs. We transfected HT-29 clones that stably overexpressed miR-375 (or miR-200, as a control) with a luciferase reporter fused to the 3′ UTR of KLF4 or KLF5. We noted a twofold inhibition in luciferase activity of the KLF5 3′ UTR after miR-375 overexpression, whereas knockdown of Dicer yielded the opposite result (**Fig. 3e**), which probably indicated direct repression of KLF5 by miR-375. A similar experiment showed that miR-375 overexpression or knockdown of Dicer had no effect on a KLF4 3′ UTR reporter (**Fig. 3e**), which suggests that KLF5 is regulated by miR-375 but KLF4 is not. We therefore propose that the goblet-cell differentiation defect in Dicer1-mutant colon could be at least in part a result of enhanced KLF5 expression due to loss of miR-375.

MicroRNAs are key regulators of gut mucosal immunity

Goblet-cell depletion is a sign of gut inflammation and a histological criterion for inflammatory bowel disease[28]. Thus, we next examined whether epithelial miR-375 regulates mucosal immunity. The T_H2 arm of cellular immunity is a chief regulator of goblet-cell maturation[1]. To determine if a specific immune pathway is deregulated in the $Dicer1^{\Delta gut}$ mice, we measured various cytokine-encoding mRNAs in the colon. We noted a lower abundance of T_H2 cytokines (interleukin 13 (IL-13), IL-4 and IL-5) in $Dicer1^{\Delta gut}$ colon tissue samples, whereas we found no change in T_H1 cytokines (**Fig. 4a** and data not shown). We therefore assessed epithelial factors that may influence T_H2 cytokines.

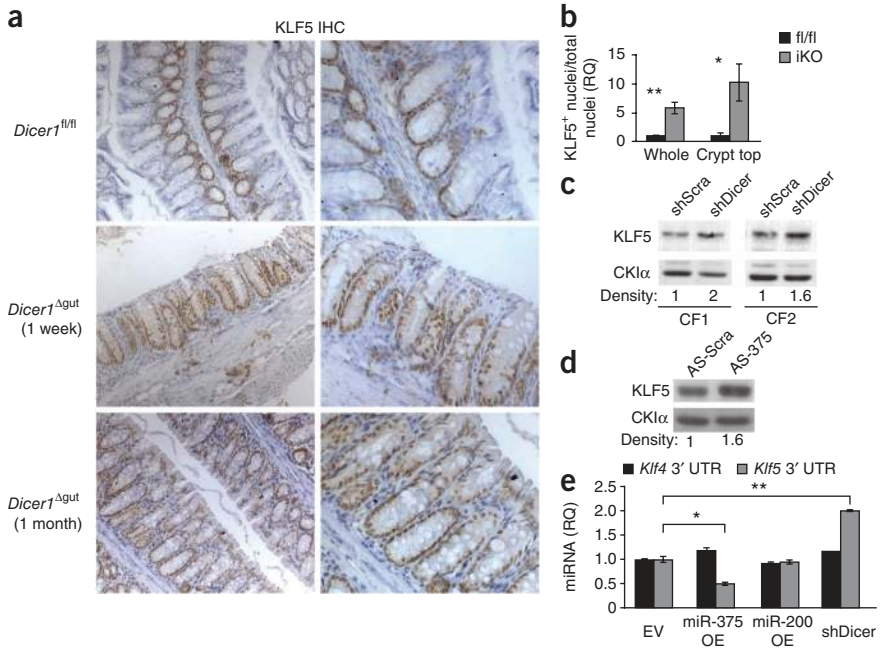

Figure 3 *Klf5* is a target of miR-375. (**a**) Immunohistochemistry (IHC) analysis of KLF5 in FFPE colon sections from *Dicer1*$^{fl/fl}$ mice and from *Dicer1*$^{\Delta gut}$ mice 1 week and 1 month after *Dicer1* ablation. Original magnification, ×100 (left) or ×200 (right). (**b**) Automated quantification of KLF5$^+$ nuclei and total nuclei throughout crypts of the entire colon (Whole) or only the top half of the crypts (the portion closer to the lumen; Crypt top), presented relative to the results of *Dicer1*$^{fl/fl}$ mice, set as 1. $*P = 0.02$ and $**P = 0.003$ (*t*-test). (**c**) Immunoblot analysis of KLF5 in differentiated HT-29 clones (CF1 and CF2) stably infected with short hairpin RNA (shRNA) specific for *Dicer* (shDicer) or scrambled shRNA sequence (shScra); CKIα serves as a control. Below lanes, densitometry. (**d**) Immunoblot analysis of KLF5 in HT-29 cells transiently transfected with 200 nM antagomir to miR-375 (AS-375) or antagomir with scrambled sequence (AS-Scra); CKIα signal serves as a control. Below lanes, densitometry. (**e**) Luciferase reporter assay of the 3′ UTRs of *Klf4* and *Klf5* in CF1 cells infected with empty vector or *Dicer*-specific shRNA or with overexpression (OE) of miR-375 or miR-200; results are presented relative to those obtained with the control reporter (empty vector) after normalization of firefly luciferase activity to renilla luciferase activity. $*P = 0.015$, miR-375 overexpression versus control, and $**P = 0.0025$, *Dicer*-specific shRNA versus control (*t*-test). Data are representative of three experiments (**a**), one experiment (**b**; mean ± s.e.m. of three mice per group), two independent experiments (**c**) or three independent experiments (**d**,**e**; mean ± s.e.m. in **e**).

Thymic stromal lymphopoietin (TSLP) is an epithelium-derived cytokine that promotes T_H2 activation while suppressing the T_H1 arm[29]. Indeed, *Dicer1*$^{\Delta gut}$ samples had less TSLP mRNA, down to 30% of the normal amount (**Fig. 4b**). Additionally, we found less mRNA and protein for RELMβ, an IEC-derived, T_H2-controlled antiparasitic factor produced mainly by goblet cells[1] (**Fig. 4b**,**c**). Notably, expression of both RELMβ mRNA and RELMβ protein was lower in miR-375-deficient mouse colon (**Fig. 4d–f**), which suggested that the RELMβ deficiency in *Dicer1*$^{\Delta gut}$ colon was due mainly to the absence of miR-375.

Studies of a variety of mouse models have demonstrated an important role for intestinal bacteria in the maintenance of colonic homeostasis[3,30]. However, we observed little to no change in goblet-cell depletion in *Dicer1*$^{\Delta gut}$ mice treated with antibiotics (**Supplementary Fig. 5a**,**b**), which suggested that their goblet-cell depletion was probably due to intrinsic epithelial defects rather than being the result of microfloral changes. Nevertheless, the altered immune phenotype of the gut indicated impairment of the epithelium–immune system relationship that is needed for the maintenance of homeostasis in the colon[4,5], which suggests that *Dicer1*$^{\Delta gut}$ mice may be vulnerable to pathogen assaults on the gut, particularly pathogens controlled by T_H2 cytokines.

Susceptibility of *Dicer1*$^{\Delta gut}$ mice to helminth infection

Trichuris muris is a pathogenic helminth of the mouse gut[1]. CD4$^+$ T_H2 cells are required for immunity to *T. muris*; its expulsion is associated with higher expression of goblet cell–derived RELMβ. We therefore used the *T. muris* infection model[31] to assess the immune competence of the gut in *Dicer1*$^{\Delta gut}$ mice. *Dicer1*$^{\Delta gut}$ mice crossed onto the C57BL/6 strain, which is a *T. muris*–resistant genetic background[32], failed to clear parasites from the gastrointestinal tract, whereas their *Dicer1*$^{fl/fl}$ littermates were resistant to the parasite (**Fig. 5a**). Furthermore, unlike their control littermates, which mounted an effective T_H2 response to the parasite, *Dicer1*$^{\Delta gut}$ mice raised an ineffective T_H1 response. This was manifested by more extensive intraepithelial T cell infiltration (**Fig. 5b**) and more mRNA for the T_H1 cytokine interferon-γ and the proinflammatory cytokines tumor necrosis factor and IL-2 in infected *Dicer1*$^{\Delta gut}$ mice than in control *Dicer1*$^{fl/fl}$ mice (**Fig. 5c**). Notably, *T. muris*–infected *Dicer1*$^{\Delta gut}$ mice failed to induce expression of the antiparasitic effector RELMβ (**Supplementary Fig. 6a**,**b**). The futility of the T_H1 immune response was further evident in the tissue edema and mucosal damage observed in the parasite-infected *Dicer1*$^{\Delta gut}$ colon (**Fig. 5b**). Overall, these immune and microbial studies suggest that *Dicer1* extinction specifically diminished functional gut T_H2 immunity.

Induction of miR-375 expression by IL-13 in IECs

IL-13 constitutes an important link between the T_H2 immune arm and differentiation of goblet cells[33]. In agreement with published studies of colorectal cancer cell lines[34], expression of the epithelium-derived T_H2 regulator RELMβ was upregulated in a time-dependent manner after stimulation of HT-29 cells with IL-13 (**Supplementary Fig. 7a**). IL-13 also induced expression of the goblet-cell maturation factor KLF4 (**Supplementary Fig. 7a**). Observation of the effects of miR-375 on innate immunity indicated possible regulation of miR-375 by IL-13, and indeed we observed more miR-375 2 h after stimulation of HT-29 cells with recombinant IL-13 (**Fig. 6a**).

It has been reported that IL-13 exerts its action through the activation of various cellular pathways, including the phosphatidylinositol-3-OH kinase (PI(3)K) pathway[33]. Indeed, the treatment of HT-29 cells with IL-13 induced phosphorylation of 4E-BP1 and S6 ribosomal protein, two well-known targets of the PI(3)K pathway[34] (**Fig. 6b**). Notably, miR-375 is expressed in pancreatic beta cells; in these cells, it is involved with glucose regulation, which is tightly associated with the PI(3)K pathway[23,35]. To determine whether the PI(3)K pathway regulates miR-375 in the colon, we used inducible gut-specific deletion of the gene encoding the PI(3)K antagonist

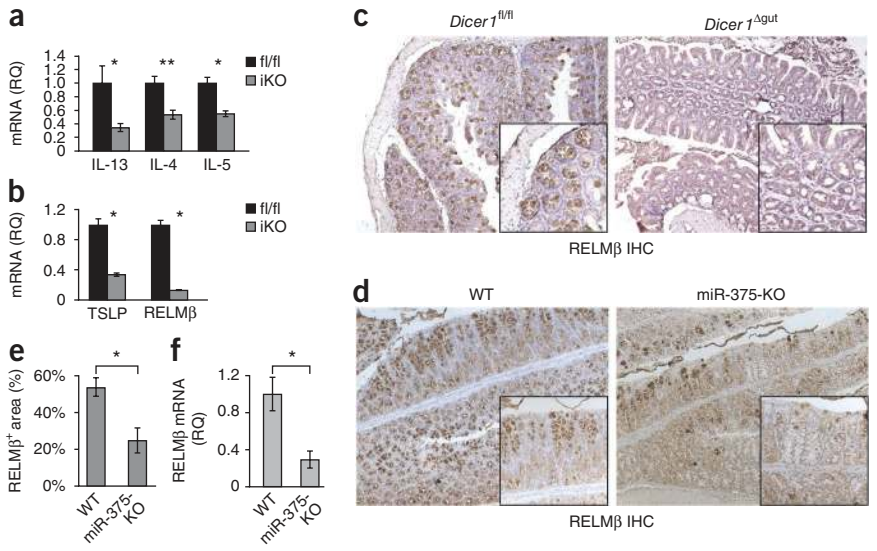

Figure 4 Immunological changes after *Dicer1* ablation in the gut. (**a**) Quantitative PCR analysis of the expression of mRNA for the T_H2 cytokines IL-4, IL-5 and IL-13 in whole-colon tissue from *Dicer1*$^{\Delta gut}$ and *Dicer1*$^{fl/fl}$ mice, presented relative to the expression in *Dicer1*$^{fl/fl}$ mice, set as 1. $^*P = 0.05$ and $^{**}P = 0.004$ (*t*-test). (**b**) Quantitative PCR analysis of the expression of TSLP mRNA and RELMβ mRNA in colonocytes isolated from *Dicer1*$^{\Delta gut}$ and *Dicer1*$^{fl/fl}$ mice, presented relative to the expression in *Dicer1*$^{fl/fl}$ mice, set as 1. $^*P < 0.05$ (*t*-test). (**c**,**d**) Immunohistochemistry of RELMβ expression in FFPE sections of the colons of *Dicer1*$^{\Delta gut}$ and *Dicer1*$^{fl/fl}$ mice (**c**) and miR-375-deficient mice and their wild-type controls (**d**). Original magnification, ×100 (main images in **c** and insets in **d**), ×400 (insets, **c**) and ×25 (main images, **d**). (**e**) Quantification of RELMβ$^+$ areas in colon sections from miR-375-deficient mice and their wild-type control littermates, presented as mean percentage of RELMβ$^+$ area. $^*P = 0.009$ (*t*-test). (**f**) RELMβ mRNA in whole-colon tissue from miR-375-deficient mice and their wild-type control littermates. $^*P = 0.006$ (*t*-test). Data are representative of two experiments (**a**,**b**,**d**; mean ± s.e.m. of three mice per group in **a**,**b**), three experiments (**c**) or one experiment (**e**,**f**; mean ± s.e.m. of five mice per group in **e** and nine wild-type mice and seven miR-375-deficient mice in **f**).

PTEN (*Pten*$^{\Delta gut}$), which results in considerable activation of PI(3)K. We found twofold more miR-375 in *Pten*$^{\Delta gut}$ IECs (**Fig. 6c**) than in control IECs (**Fig. 6d**). This suggests that activation of the PI(3)K pathway induces miR-375 *in vivo*. The greater abundance of miR-375 in *Pten*$^{\Delta gut}$ colon was associated with notably more goblet cells (**Fig. 6e**) and higher expression of the goblet-cell marker Gob5 (**Fig. 6c**), as well as with higher expression of RELMβ (**Fig. 6c**,**e**). These *Pten*$^{\Delta gut}$ characteristics were in contrast to the *Dicer1*$^{\Delta gut}$ phenotype, which supports the idea of a potential role for the PI(3)K pathway in the control of goblet-cell differentiation by miRNA.

Athymic nude mice, which lack T cells, had low RELMβ expression (**Fig. 6f**), resembling the *Dicer1*$^{\Delta gut}$ phenotype (**Fig. 4c**). Like *Dicer1*$^{\Delta gut}$ mice, nude mice are also vulnerable to gut helminths because of an ineffective T_H2 response[32]. We therefore thought that the nude strain would be a suitable model for testing T cell control of miR-375 in the colon. Indeed, the colons of nude mice had less miR-375 than did the colons of wild-type mice, whereas the expression of other miRNAs was unaffected (**Fig. 6g**), which indicated that miR-375 is probably subjected to T cell control, possibly via IL-13. As IL-13 has been shown to signal through the PI(3)K pathway[33], we sought to determine whether non-immune activation of this pathway in nude mice would induce miR-375 expression and goblet-cell differentiation. We therefore crossed *Dicer1*$^{\Delta gut}$ mice onto the nude genetic background, creating a nude *Dicer1*$^{\Delta gut}$ line. We treated nude mice and nude *Dicer1*$^{\Delta gut}$ mice with the PTEN inhibitor bpV(phen) (bis-peroxovanadium 1,10-phenanthroline) to activate the PI(3)K pathway. This treatment resulted in more miR-375, more goblet cells and higher RELMβ expression in nude mice, whereas nude *Dicer1*$^{\Delta gut}$ mice failed to respond to bpV(phen) (**Fig. 6f**,**g** and **Supplementary Fig. 8**). These

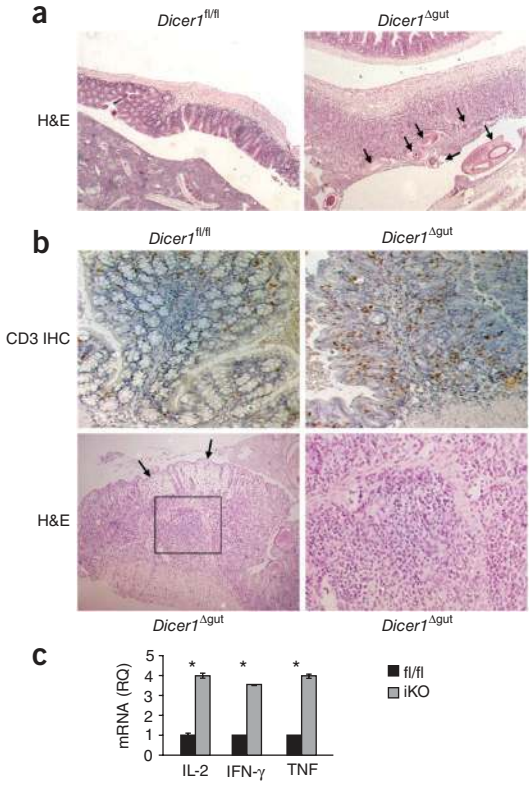

Figure 5 Deletion of *Dicer1* in the gut epithelium results in ineffective inflammatory responses to and susceptibility to *T. muris*. (**a**) Hematoxylin and eosin (H&E) staining of FFPE colon sections from *Dicer1*$^{\Delta gut}$ and *Dicer1*$^{fl/fl}$ mice 30 d after infection with *T. muris* (arrows). Original magnification, ×25. (**b**) FFPE colon sections from *Dicer1*$^{\Delta gut}$ and *Dicer1*$^{fl/fl}$ mice, stained for CD3 (T lymphocytes) 30 d after *T. muris* infection (top), and hematoxylin and eosin staining of FFPE colon sections of *T. muris*–infected *Dicer1*$^{\Delta gut}$ mice, showing parasitic invasion of colonic wall with tissue damage and edema (arrows; bottom left) and inflammatory infiltrates (bottom right; enlargement of area outlined at left). Original magnification, ×100 (top), ×25 (bottom left) or ×400 (bottom right). (**c**) Analysis of mRNA for IL-2, interferon-γ (INF-γ) and tumor necrosis factor (TNF) in whole-colon tissue from *Dicer1*$^{\Delta gut}$ and *Dicer1*$^{fl/fl}$ mice 30 d after *T. muris* infection, presented relative to the expression in *Dicer1*$^{fl/fl}$ mice, set as 1. $^*P < 0.03$ (*t*-test). Data are representative of one experiment with three mice per group (mean ± s.e.m. in **c**).

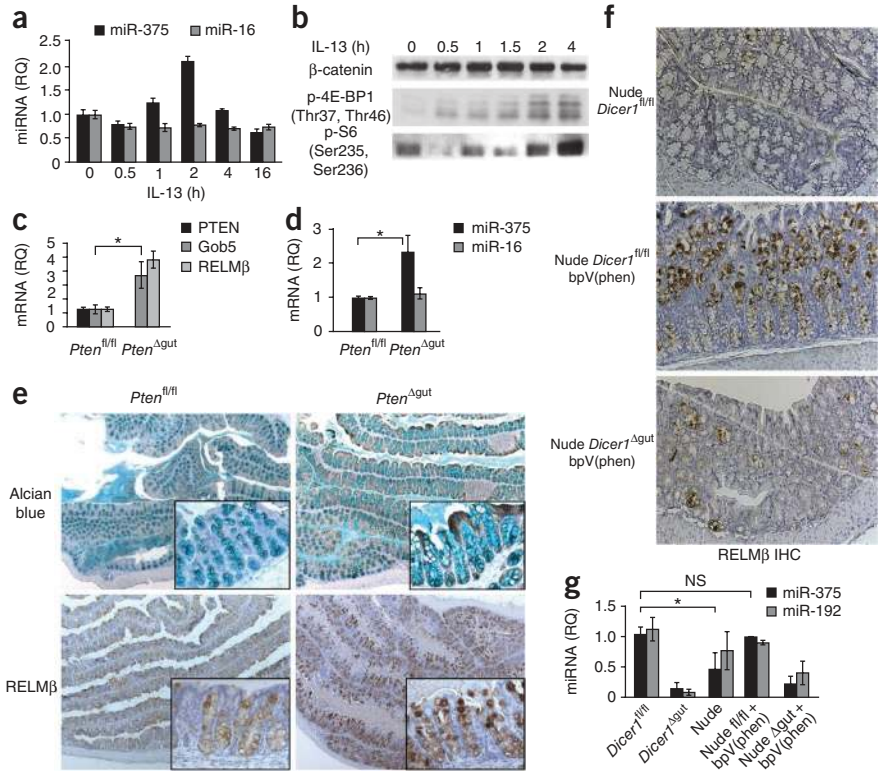

Figure 6 IL-13 induces miR-375 expression via the PI(3)K pathway. (**a**) Quantitative PCR analysis of miR-375 and miR-16 in HT-29 cells after the administration of recombinant human IL-13 (10 nM). (**b**) Immunoblot analysis of activation of the PI(3)K pathway in HT-29 cells stimulated with IL-13 (10 nM), probed with antibodies to 4E-BP1 phosphorylated (p-) at Thr37 and Thr46 (middle) and S6 phosphorylated at Ser235 and Ser236 (bottom); β-catenin serves as a loading control (top). (**c**,**d**) Expression of PTEN mRNA, Gob5 mRNA and RELMβ mRNA (**c**) and of miR-375 and miR-16 (**d**) in colonocytes from *Pten*$^{fl/fl}$ and *Pten*$^{\Delta gut}$ mice. Results are presented relative to the expression in *Pten*$^{fl/fl}$ mice, set as 1. *$P < 0.03$ (**c**) or 0.02 (**d**; *t*-test). (**e**) FFPE colon sections from *Pten*$^{fl/fl}$ and *Pten*$^{\Delta gut}$ mice stained with Alcian blue (top) and analyzed by immunohistochemistry for RELMβ (bottom). Original magnification, ×25 (main images) or ×200 (insets). (**f**) Immunohistochemistry of RELMβ in FFPE colon sections from nude *Dicer1*$^{fl/fl}$ mice and nude *Dicer1*$^{\Delta Gut}$ mice left untreated (top) or treated with bpV(phen) (middle and bottom). Original magnification, ×200. (**g**) Expression of miR-375 and miR-192 in colonocytes from *Dicer1*$^{fl/fl}$, *Dicer1*$^{\Delta gut}$ and nude mice left untreated, and from nude *Dicer1*$^{fl/fl}$ mice (Nude fl/fl) and nude *Dicer1*$^{\Delta gut}$ mice (Nude ΔDgut) treated with bpV(phen). NS, not significant; *$P = 0.008$ (*t*-test). Data are representative of two independent experiments (**a**,**b**; mean ± s.e.m. in **a**) or one experiment (**c**–**g**; mean ± s.e.m. of three (**c**) or four (**d**,**g**) mice per group).

results indicate that the miRNA pathway is an essential intermediate in the induction of goblet cells and RELMβ via PI(3)K activation and that non-immune PI(3)K activation can replace IL-13 in restoring functional miR-375 and RELMβ in nude mice. Together these studies (**Fig. 6**) demonstrate how immune and non-immune signals might control goblet differentiation and how they might raise goblet cell innate immunity effectors by inducing epithelial miR-375; it remains to be explained how the epithelium facilitates a T_H2 response via miRNA activation.

Enhanced TSLP expression via miR-375

Dicer1$^{\Delta gut}$ mice had a lower abundance of epithelial TSLP, which could have been responsible for their impaired T_H2 activity (**Fig. 4b**). To determine whether miR-375 induces TSLP expression and hence the T_H2 response, we assessed the expression of miR-375 and TSLP mRNA after IL-13 stimulation in HT-29 cells and found a concomitant increase in both after 2 h of stimulation (**Figs. 6a** and **7a**). To rule out the possibility that IL-13 induces TSLP independently of miR-375, we assessed cytokine expression in HT-29 cells depleted of miR-375. Upregulation of TSLP mRNA and protein by IL-13 was inhibited by knockdown of miR-375 (**Fig. 7a**,**b**). Likewise, miR-375 overexpression in HT-29 cells enhanced TSLP mRNA expression (**Fig. 7c**). Concordantly, we found that the goblet cell–like clone CF1 had higher expression of TSLP mRNA than did the enterocyte-like clone CF2 (**Fig. 7d**). These results suggest that miR-375 is both an activator and a downstream target of the T_H2 response, in which the activator function is mediated via the induction of TSLP (**Supplementary Fig. 9**).

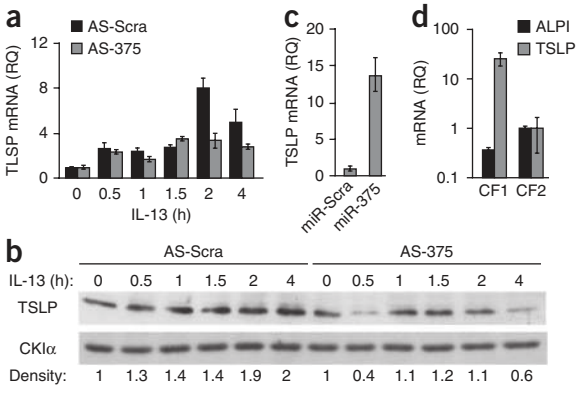

Figure 7 Regulation of TSLP expression by miR-375. (**a**) Time course of TSLP mRNA expression in HT-29 cells transfected with antagomir with scrambled sequence or specific for miR-375, then stimulated with IL-13 (10 nM); results are presented relative to the expression in unstimulated cells transfected with scrambled antagomir, set as 1. (**b**) Immunoblot analysis of TSLP in HT-29 cells transfected and treated as in **a**; CKIα serves as a loading control. Below, densitometry. (**c**) TSLP mRNA in HT-29 cells stably infected for overexpression of miRNA with scrambled sequence or miRNA-375; results are presented relative to the abundance of TSLP mRNA in cells infected with scrambled miRNA, set as 1. (**d**) TSLP mRNA and alkaline phosphatase mRNA in differentiated HT-29 clones (CF1 and CF2), presented (in a logarithmic scale) relative to the expression in CF2, set as 1. Data are representative of three (**a**,**b**) or two (**c**,**d**) experiments (mean ± s.e.m. in **a**,**c**,**d**).

DISCUSSION

It is well documented that miRNAs contribute to the regulation of diverse biological processes, including cell proliferation, cell death, differentiation, organogenesis, tumorigenesis, immunity and more[7,8]. Using a mouse model of inducible inactivation of *Dicer1* in the gut (*Dicer1*$^{\Delta gut}$), we have shown here that miRNAs are also involved in the differentiation and homeostasis of the gut mucosa. Deletion of *Dicer1* in adult colon epithelium had no effect on apoptosis and tissue renewal but had a substantial effect on one particular cell type, goblet cells, which suggests that miRNAs regulate goblet-cell differentiation. Specific miRNAs are involved in differentiation processes in hematopoietic lineages, muscle and pancreas development[10,11,35]. We identified a specific miRNA, miR-375, that seemed to have an important role in the T_H2 response of gut mucosal immunity and thus may be involved in goblet-cell differentiation and function. We found high expression of miR-375 in colonic epithelium, and its overexpression in HT-29 colorectal cancer cells facilitated goblet cell–specific gene expression in the absence of other mature miRNAs, which indicates a particular role for this miRNA in intestinal epithelium differentiation. Although we did not find goblet-cell depletion in miR-375-deficient mice, as in *Dicer1*$^{\Delta gut}$ (shown here and in ref. 36), we detected lower abundance of the T_H2-controlled goblet cell marker Gob5 (ref. 37) in the gut of mice with germline deficiency in miR-375. This phenotypic difference could result from the involvement of other miRNAs in goblet-cell differentiation or compensatory mechanisms in a constitutive knockout mouse model. Therefore, appreciation of the full scope of the importance of miR-375 in gut homeostasis will probably require a model of gut-specific inducible deficiency in miR-375. Nevertheless, and in line with the *Dicer1*$^{\Delta gut}$ phenotype, we observed in the colon of miR-375-deficient mice much less RELMβ, the main antiparasitic effector of goblet cells[1], which possibly explains part of the mucosal immune deficit of *Dicer1*$^{\Delta gut}$ mice. To our knowledge, this is the first linkage of a specific miRNA with an antiparasitic immune response.

We addressed the mode of action of miRNAs in the colon by examining potential regulators of goblet differentiation. Among these were KLF4 and KLF5, members of the KLF family. KLF4 is a key participant in goblet-cell differentiation and is normally located in the upper portion of the colonic crypt. In contrast, KLF5 promotes proliferation and suppresses differentiation and is accordingly located at the bottom of the crypt[26]. *Klf4* ablation in mice results in massive depletion of goblet cells in the colon[38]. These two factors are known to antagonize each other's activity at the *Klf4* promoter, where KLF4 promotes its own expression and KLF5 represses the promoter activity[26]. Although both factors have a potential miR-375 target sequence, we found that only *Klf5* was regulated by miR-375, which suggests context-dependent regulation[39,40]. Concordantly, KLF5 protein expression gradually increased, expanding to cover the entire span of the colonic crypts after *Dicer1* ablation. We therefore propose that miR-375 facilitates goblet-cell maturation by suppressing KLF5 protein. It is possible, however, that other miRNA targets also have a role in the observed phenotype of the *Dicer1*$^{\Delta gut}$ mouse.

Goblet cells fulfill an important role in gut mucosal immunity; their secretions are part of the gut physical barrier and contain essential antimicrobial agents[1]. Goblet cells increase in number in response to intestinal infection, particularly by parasites; this is referred to as 'goblet hyperplasia'[41]. The induction of goblet-cell hyperplasia is known to depend on hyperactivation of the T_H2 response[41]. Failure to produce mature goblet cells and/or sufficient RELMβ may compromise the immune balance of the gut, resulting in chronic gut inflammation elicited by proinflammatory cytokines[29]. Assessment of the *Dicer1*$^{\Delta gut}$ mucosal immune status showed that these mice had a lower abundance of T_H2 cytokines (IL-4, IL-5 and IL-13). TSLP, a known regulator of the mucosal T_H2 response, is an epithelium-derived cytokine first described in the context of the growth of early B cell and T cell progenitors[42]. Mounting data indicate a crucial role for TSLP in epithelium–immune system crosstalk that promotes a T_H2 response, by two possibly complementary mechanisms: suppression of T_H1 responses[4], and recruitment of basophils, the main antigen-presenting cells in the T_H2 response of the gut[43–45]. The importance of TSLP in suppressing T_H1 response–associated pathologies is emphasized by the undetectable TSLP in 70% of patients with Crohn's disease, which, like other inflammatory bowel diseases, is distinguished by a dominant T_H1 response[46]. Consistent with those studies, we observed less TSLP mRNA in *Dicer1*$^{\Delta gut}$ mice and greater susceptibility of *Dicer1*$^{\Delta gut}$ mice to *T. muris* infection. Hence, epithelial miRNAs may regulate mucosal immunity by modulating TSLP, a key mediator of epithelial cell–T cell crosstalk.

Studies have linked miRNAs to signaling-induced cellular differentiation. For example, miR-155 is induced by lipopolysaccharide stimulation to promote the differentiation of naive helper T cells into T_H1 cells[47]. In search of a possible miR-375 inducer, we investigated IL-13, a T_H2 mediator with a dominant role in the expulsion of helminths from the gut[48]. Our *in vitro* data suggested that IL-13 induces miR-375, generating two outcomes: first, goblet cell maturation, inclusive of the antiparasitic cytokine RELMβ; and second, upregulation of TSLP. Inhibition of miR-375 abrogated the induction of TSLP in response to IL-13, which indicated a positive feedback mechanism for activation of the T_H2 response and goblet-cell differentiation. The gene encoding TSLP has been shown to be a target of NF-κB[4]. Accordingly, we propose that whereas basal TSLP expression is regulated by NF-κB, possibly in response to the normal gut microflora, parasite invasion boosts TSLP expression via IL-13-mediated induction of miR-375.

IL-13 activates the PI(3)K pathway[33], which suggests that this pathway mediates the induction of miR-375 in response to T_H2 cytokines. We found that *Pten*$^{\Delta gut}$ mice with constitutively more PI(3)K activity in the gut had higher miR-375 expression and enhanced goblet-cell maturation. Conversely, immunodeficient nude mice, which lack T cells, had less miR-375 and less of the intestinal goblet cell–specific T_H2 effector RELMβ. Administering the PTEN inhibitor bpV(phen) to nude mice augmented intestinal miR-375 expression up to the expression in immunocompetent mice and restored RELMβ expression. Notably, we observed no restoration of goblet cells or RELMβ after treatment of nude *Dicer1*$^{\Delta gut}$ mice with bpV(phen), which suggests that miRNA activity is a necessary intermediate in the PI(3)K-mediated regulation of goblet cells by the T_H2 repsonse. It is therefore likely that the induction of miR-375 in the early T_H2 response via PI(3)K activation results in upregulation of TSLP, which in turn further accentuates the T_H2 response. Once miR-375 is inhibited (such as by knockdown of miR-375 or by inactivation of *Dicer1*), TSLP expression will not increase sufficiently and the T_H2 response may decrease below the threshold necessary to sustain parasite resistance.

Our studies have shown that epithelial miRNAs regulate the expression of cytokines that generate crosstalk between gut epithelial cells and the mucosal immune system. This circuit maintains an important link between the T_H2 immune arm and gut mucosal resistance to parasite infection. Failure to tie this link, as in *Dicer1*$^{\Delta gut}$ mice, predisposes the organism to parasitic infections and T_H1-dominated chronic inflammation. We specified one miRNA that probably has a key role in this complex relationship, yet the distinction between the mucosal phenotypes of *Dicer1*$^{\Delta gut}$ mice and miR-375-deficient mice leaves room for the involvement of other miRNAs in epithelium–immune system

crosstalk. Further support for the idea that miR-375 is important in the maintenance of gut homeostasis has been provided by studies of human inflammatory bowel disease showing much less miR-375 in the colons of patients with active ulcerative colitis[21]. Increasing miR-375, either directly or through pharmacological intervention, may therefore ameliorate T_H1-mediated inflammatory bowel diseases, whereas antagonizing miR-375 activity may be valuable for the treatment of T_H2 pathologies, such as asthma.

METHODS

Methods and any associated references are available in the online version of the paper at http://www.nature.com/natureimmunology/.

Note: Supplementary information is available on the Nature Immunology website.

ACKNOWLEDGMENTS

We thank S. Robine (Institut Curie, Centre National de la Recherche Scientifique) for Villin Cre-ER^{T2} mice; C.J. Tabin (Harvard Medical School) for *Dicer1*$^{fl/fl}$ mice; P.P. Pandolfi (Harvard Medical School) for *Pten*$^{fl/fl}$ mice; K. Rajewsky (Harvard Medical School) for antibody to Dicer; I. Ben-Porath (Hebrew University) for reagents; H. Clevers for IEC-isolation protocols; Y. Smith for assistance in genomic data analysis; M. Leshets and I. Burstain for handling the confocal microscopy; and R. Goldstein for critical review of the manuscript. Supported by the Israel Science Foundation, Israel Cancer Research Fund, Hadassah Medical Center (A.L.), the German-Israeli Foundation, the Dr. Miriam and Sheldon G. Adelson Medical Research Foundation and the Crohn's & Colitis Foundation of America.

AUTHOR CONTRIBUTIONS

M.B. and A.L. did experiments, analyzed data, provided ideas and contributed to the writing of the manuscript; M.S. did experiments, analyzed data and contributed ideas; I.A., H.M., F.Z. and E.H. did experiments and analyzed data; G.C. provided bioinformatics assistance; S.K.-R., T.A.-S., M.N.P., D.A., M.D.W. and E.H. provided ideas and experimental reagents; Z.B. and E.H. contributed to preparing the manuscript; and Y.B.-N. and E.P. directed the study, contributed to the writing of the manuscript and supervised the work.

COMPETING FINANCIAL INTERESTS

The authors declare no competing financial interests.

Published online at http://www.nature.com/natureimmunology/.
Reprints and permissions information is available online at http://npg.nature.com/reprintsandpermissions/.

1. Artis, D. *et al.* RELMβ/FIZZ2 is a goblet cell-specific immune-effector molecule in the gastrointestinal tract. *Proc. Natl. Acad. Sci. USA* **101**, 13596–13600 (2004).
2. Lee, J. *et al.* Maintenance of colonic homeostasis by distinctive apical TLR9 signalling in intestinal epithelial cells. *Nat. Cell Biol.* **8**, 1327–1336 (2006).
3. Nenci, A. *et al.* Epithelial NEMO links innate immunity to chronic intestinal inflammation. *Nature* **446**, 557–561 (2007).
4. Zaph, C. *et al.* Epithelial-cell-intrinsic IKK-β expression regulates intestinal immune homeostasis. *Nature* **446**, 552–556 (2007).
5. Taylor, B.C. *et al.* TSLP regulates intestinal immunity and inflammation in mouse models of helminth infection and colitis. *J. Exp. Med.* **206**, 655–667 (2009).
6. Schickel, R., Boyerinas, B., Park, S.M. & Peter, M.E. MicroRNAs: key players in the immune system, differentiation, tumorigenesis and cell death. *Oncogene* **27**, 5959–5974 (2008).
7. Bartel, D.P. MicroRNAs: genomics, biogenesis, mechanism, and function. *Cell* **116**, 281–297 (2004).
8. Bushati, N. & Cohen, S.M. microRNA functions. *Annu. Rev. Cell Dev. Biol.* **23**, 175–205 (2007).
9. Landgraf, P. *et al.* A mammalian microRNA expression atlas based on small RNA library sequencing. *Cell* **129**, 1401–1414 (2007).
10. Koralov, S.B. *et al.* Dicer ablation affects antibody diversity and cell survival in the B lymphocyte lineage. *Cell* **132**, 860–874 (2008).
11. O'Rourke, J.R. *et al.* Essential role for Dicer during skeletal muscle development. *Dev. Biol.* **311**, 359–368 (2007).
12. Andl, T. *et al.* The miRNA-processing enzyme dicer is essential for the morphogenesis and maintenance of hair follicles. *Curr. Biol.* **16**, 1041–1049 (2006).
13. Harfe, B.D., McManus, M.T., Mansfield, J.H., Hornstein, E. & Tabin, C.J. The RNaseIII enzyme Dicer is required for morphogenesis but not patterning of the vertebrate limb. *Proc. Natl. Acad. Sci. USA* **102**, 10898–10903 (2005).
14. Barker, N. *et al.* Identification of stem cells in small intestine and colon by marker gene Lgr5. *Nature* **449**, 1003–1007 (2007).
15. van der Flier, L.G. & Clevers, H. Stem cells, self-renewal, and differentiation in the intestinal epithelium. *Annu. Rev. Physiol.* **71**, 241–260 (2009).
16. Velcich, A. *et al.* Patterns of expression of lineage-specific markers during the in vitro-induced differentiation of HT29 colon carcinoma cells. *Cell Growth Differ.* **6**, 749–757 (1995).
17. Augeron, C. & Laboisse, C.L. Emergence of permanently differentiated cell clones in a human colonic cancer cell line in culture after treatment with sodium butyrate. *Cancer Res.* **44**, 3961–3969 (1984).
18. Lee, Y. *et al.* The nuclear RNase III Drosha initiates microRNA processing. *Nature* **425**, 415–419 (2003).
19. Cummins, J.M. *et al.* The colorectal microRNAome. *Proc. Natl. Acad. Sci. USA* **103**, 3687–3692 (2006).
20. Kida, Y. & Han, Y.P. MicroRNA expression in colon adenocarcinoma. *J. Am. Med. Assoc.* **299**, 2628 (2008).
21. Wu, F. *et al.* MicroRNAs are differentially expressed in ulcerative colitis and alter expression of macrophage inflammatory peptide-2α. *Gastroenterology* **135**, 1624–1635 e1624 (2008).
22. Avnit-Sagi, T., Kantorovich, L., Kredo-Russo, S., Hornstein, E. & Walker, M.D. The promoter of the pri-miR-375 gene directs expression selectively to the endocrine pancreas. *PLoS ONE* **4**, e5033 (2009).
23. Poy, M.N. *et al.* miR-375 maintains normal pancreatic alpha- and beta-cell mass. *Proc. Natl. Acad. Sci. USA* **106**, 5813–5818 (2009).
24. Shroyer, N.F., Wallis, D., Venken, K.J., Bellen, H.J. & Zoghbi, H.Y. Gfi1 functions downstream of Math1 to control intestinal secretory cell subtype allocation and differentiation. *Genes Dev.* **19**, 2412–2417 (2005).
25. Friedman, R.C., Farh, K.K., Burge, C.B. & Bartel, D.P. Most mammalian mRNAs are conserved targets of microRNAs. *Genome Res.* **19**, 92–105 (2009).
26. McConnell, B.B., Ghaleb, A.M., Nandan, M.O. & Yang, V.W. The diverse functions of Kruppel-like factors 4 and 5 in epithelial biology and pathobiology. *Bioessays* **29**, 549–557 (2007).
27. Dang, D.T., Zhao, W., Mahatan, C.S., Geiman, D.E. & Yang, V.W. Opposing effects of Kruppel-like factor 4 (gut-enriched Kruppel-like factor) and Kruppel-like factor 5 (intestinal-enriched Kruppel-like factor) on the promoter of the Kruppel-like factor 4 gene. *Nucleic Acids Res.* **30**, 2736–2741 (2002).
28. Van der Sluis, M. *et al.* Muc2-deficient mice spontaneously develop colitis, indicating that MUC2 is critical for colonic protection. *Gastroenterology* **131**, 117–129 (2006).
29. Saenz, S.A., Taylor, B.C. & Artis, D. Welcome to the neighborhood: epithelial cell-derived cytokines license innate and adaptive immune responses at mucosal sites. *Immunol. Rev.* **226**, 172–190 (2008).
30. Kelly, D., Conway, S. & Aminov, R. Commensal gut bacteria: mechanisms of immune modulation. *Trends Immunol.* **26**, 326–333 (2005).
31. Panesar, T.S. The early phase of tissue invasion by *Trichuris muris* (nematoda: Trichuroidea). *Z. Parasitenkd.* **66**, 163–166 (1981).
32. Cliffe, L.J. & Grencis, R.K. The *Trichuris muris* system: a paradigm of resistance and susceptibility to intestinal nematode infection. *Adv. Parasitol.* **57**, 255–307 (2004).
33. Wang, M.L. *et al.* Immune-mediated signaling in intestinal goblet cells via PI3-kinase- and AKT-dependent pathways. *Am. J. Physiol. Gastrointest. Liver Physiol.* **295**, G1122–G1130 (2008).
34. Langlois, M.J. *et al.* Epithelial phosphatase and tensin homolog regulates intestinal architecture and secretory cell commitment and acts as a modifier gene in neoplasia. *FASEB J.* **23**, 1835–1844 (2009).
35. Poy, M.N. *et al.* A pancreatic islet-specific microRNA regulates insulin secretion. *Nature* **432**, 226–230 (2004).
36. McKenna, L.B. *et al.* MicroRNAs control intestinal epithelial differentiation, architecture, and barrier function. *Gastroenterology* **139**, 1654–1664 (2010).
37. Hauber, H.P., Lavigne, F., Hung, H.L., Levitt, R.C. & Hamid, Q. Effect of Th2 type cytokines on hCLCA1 and mucus expression in cystic fibrosis airways. *J. Cyst. Fibros.* **9**, 277–279 (2010).
38. Katz, J.P. *et al.* The zinc-finger transcription factor Klf4 is required for terminal differentiation of goblet cells in the colon. *Development* **129**, 2619–2628 (2002).
39. Grimson, A. *et al.* MicroRNA targeting specificity in mammals: determinants beyond seed pairing. *Mol. Cell* **27**, 91–105 (2007).
40. Kertesz, M., Iovino, N., Unnerstall, U., Gaul, U. & Segal, E. The role of site accessibility in microRNA target recognition. *Nat. Genet.* **39**, 1278–1284 (2007).
41. Ishikawa, N., Wakelin, D. & Mahida, Y.R. Role of T helper 2 cells in intestinal goblet cell hyperplasia in mice infected with *Trichinella spiralis*. *Gastroenterology* **113**, 542–549 (1997).
42. Friend, S.L. *et al.* A thymic stromal cell line supports in vitro development of surface IgM$^+$ B cells and produces a novel growth factor affecting B and T lineage cells. *Exp. Hematol.* **22**, 321–328 (1994).
43. Perrigoue, J.G. *et al.* MHC class II–dependent basophil–CD4$^+$ T cell interactions promote T_H2 cytokine–dependent immunity. *Nat. Immunol.* **10**, 697–705 (2009).
44. Sokol, C.L. *et al.* Basophils function as antigen-presenting cells for an allergen-induced T helper type 2 response. *Nat. Immunol.* **10**, 713–720 (2009).
45. Wynn, T.A. Basophils trump dendritic cells as APCs for T_H2 responses. *Nat. Immunol.* **10**, 679–681 (2009).
46. Rimoldi, M. *et al.* Intestinal immune homeostasis is regulated by the crosstalk between epithelial cells and dendritic cells. *Nat. Immunol.* **6**, 507–514 (2005).
47. Tili, E. *et al.* Modulation of miR-155 and miR-125b levels following lipopolysaccharide/TNF-α stimulation and their possible roles in regulating the response to endotoxin shock. *J. Immunol.* **179**, 5082–5089 (2007).
48. Bancroft, A.J., Artis, D., Donaldson, D.D., Sypek, J.P. & Grencis, R.K. Gastrointestinal nematode expulsion in IL-4 knockout mice is IL-13 dependent. *Eur. J. Immunol.* **30**, 2083–2091 (2000).

ONLINE METHODS

Mouse procedures. Mice were housed and cared for under specific pathogen–free conditions, and all animal procedures were approved by the Animal Care and Use Committee of the Hebrew University of Jerusalem (details of mouse experiments, **Supplementary Methods**). Mice with conditional deletion of *Dicer1*$^{fl/fl}$ were generated in the laboratory of C.J. Tabin; *Pten*$^{fl/fl}$ mice were from P.P. Pandolfi; mice with germline knockout of miR-375 have been described[23]; mice with transgenic expression of Cre recombinase fused to a mutant estrogen receptor, driven by the enterocyte-specific promoter of the gene encoding Villin (Villin-Cre ER^{T2}) were provided by S. Robine; mice carrying a germline-transmitted transgene containing the miR-375 promoter driving expression of enhanced green fluorescent protein were generated by standard procedures with a published vector[22]; nude mice were from the Jackson Laboratory.

Histochemistry and immunohistochemistry. All tissues were fixed for 24 h in 4% (wt/vol) formaldehyde, embedded in paraffin and cut into sections 5 μm in thickness for staining with hematoxylin and eosin and immunostaining. Sections were deparaffinized by standard techniques. Sections were then incubated overnight at 4 °C with primary antibodies at the following dilutions: antibody to Muc2 (anti-Muc2), 1:100 (sc-59859; Santa Cruz); anti-KLF5, 1:200 (AF3758; R&D); anti-RELMβ, 1:200 (500-P215; PeproTech); anti-PTEN, 1:200 (9559; Cell Signaling); anti-CD3, 1:100 (RM-9107; Neomarkers); and antibody to cleaved caspase-3, 1:100 (9661; Cell Signaling). For Alcian blue staining, deparaffinized and rehydrated slides were incubated for 30 min in Alcian blue solution, pH 2.5, and were counterstained with nuclear Fast Red. For periodic acid–Schiff staining, 0.5% (wt/vol) periodic acid was added to cell culture plates for 5 min, followed by incubation for 30 min with Schiff's reagent. The frequency of goblet cells positive for Alcian blue was assessed with the Gensight module of the Ariol SL-50 automated scanning microscope and image-analysis system according to the manufacturer's instructions (Applied Imaging). For each sample, the average ratio of positive area to total nuclei area was determined in 30 arbitrary chosen mucosal fields. For KLF5 analysis, the ratio of positive nuclei area to total nuclei area was determined separately for the entire crypt area or the top half of the crypt area of the colonic mucosa. The extent of RELMβ expression in the colon was assessed by an researcher 'blinded' to mouse genotype.

TdT-mediated dUTP nick end labeling assay. An *In Situ* Cell Death Detection kit was used for TdT-mediated dUTP nick end labeling according to the manufacturer's instructions (Roche). FFPE colon sections were deparaffinized and then treated for 9 min at 25 °C with nuclease-free proteinase K (Roche). TdT enzyme diluted in labeling solution was applied to the tissues for 1 h at 37 °C. Samples were counterstained with Hoechst 33342 (Invitrogen).

Immunofluorescence. Small bowel and colon were fixated in 4% (wt/vol) paraformaldehyde, incubated in solution of 30% (wt/vol) sucrose and frozen at −80 °C in optimum cutting temperature compound (Sakura). Sections 10 μm in thickness were cut on a Cryostat (Leica) and kept at −20 °C. Samples were counterstained with Hoechst 33342 (Invitrogen). Fluorescent mounting medium (Dako) was used to prevent fading of stained samples inspected by confocal microscopy.

Laser-capture microdissection. Freshly prepared FFPE colonic sections were processed by laser-capture microdissection according to the manufacturer's instructions (P.A.L.M. Microlaser Technologies).

Quantitative PCR. Total RNA was extracted from cell pellets or homogenized whole colon with an miRNeasy Kit (Qiagen) and was subjected to reverse transcription with m-MLV-RT (Invitrogen). Quantitative mRNA expression was analyzed by real-time PCR (ABI 7900), with SYBR Green (Invitrogen). RT-PCR primers were designed for an exon-exon boundary in all transcripts when possible. *Ndufb9* (encoding mouse NADH dehydrogenase (ubiquinone) 1β) and *UBC* (encoding human ubiquitin C) served as endogenous reference genes.

Quantitative PCR analysis of mature miRNA was done according to a published protocol[49]. U6 small nuclear RNA served as the endogenous reference gene. Primer sequences are in the **Supplementary Methods** and **Supplementary Table 1**.

Immunoblot analysis. Proteins were extracted by standard techniques. Primary antibodies and dilutions were as follows: anti-Dicer, 1:1,000 (I96; from K. Rajewsky); anti-CKIα, 1:100 (sc-6477; Santa Cruz); anti-KLF5, 1:1,000 (AF3758; R&D Systems); anti-β-catenin, 1:2,500 (610153; BD transduction); antibody to 4E-BP1 phosphorylated at Thr37 and Thr46, 1:1,000 (2855; Cell Signaling); antibody to S6 phosphorylated at Ser235 and Ser236, 1:1,000 (2211; Cell Signaling); anti-TSLP, 1:2,000 (500-P258; PeproTech).

Lentivirus constructs and transduction. Lentiviruses were produced by transient three-plasmid transfection as described[50]. These viruses were used to transduce HT-29 cells in the presence of polybrene (5 μg/ml). Oligonucleotides encoding *Drosha*-specific shRNA were annealed and inserted into the lentiviral vector SIN18-pRLL-hEFIα p-eGFP-WRPE45 as described[50]; oligonucleotides encoding miR-375, miR-16, miR-200c and shRNA with a scrambled sequence were annealed and inserted into the pLKO construct (sequences, **Supplementary Methods** and **Supplementary Table 2**). The pLKO construct containing *Dicer*-specific shRNA was from Open Biosystems (TRCN0000051261).

Luciferase reporter assay. Full-length *Klf4* 3′ UTR containing the miR-375 site or 500 nucleotides of the 3′ UTR of *Klf5* containing the miR-375 site were fused to the coding region of the gene encoding firefly luciferase (pGL3 control vector; Promega). Primers for PCR cloning are in the **Supplementary Methods** and **Supplementary Table 3**. These procedures were done as described[50].

Differentiation of HT-29 cells, clone isolation and cytokine experiments. Cells (2×10^6) were differentiated *in vitro* as described[17]. Specific goblet-cell and enterocyte clones were isolated by the limiting-dilution plating technique. After *in vitro* differentiation, HT-29 cells were diluted in culture medium to yield a final density of 30 cells per ml and were dispensed into wells of 96-well microtest plates (Falcon). Each well was inoculated with 50 μl cell suspension, yielding an average density of 1.5 cells per well. Each subclone was analyzed by staining with periodic acid–Schiff and for specific markers, as well as by quantitative PCR. For IL-13 stimulation, 2 d after plating of HT-29 cells, IL-13 (10 nM; PeproTech) was added to the standard cell culture medium for the appropriate time.

Antagomir-based knockdown of miR-375. HT-29 cells were treated with 2′-O-methyl antagomir to miR-375 or control antagomir with three locked nucleotide acid positions (synthesized by Integrated DNA Technologies; sequences, **Supplementary Methods** and **Supplementary Table 4**). Additionally, fluorescein-labeled antagomir to miR-375 and scrambled control antagomir were used (Exiqon). Cells were transfected with the modified antagomirs at a final concentration of 200 nM through the use of LT1 transfection reagent (Mirus).

49. Shi, R. & Chiang, V.L. Facile means for quantifying microRNA expression by real-time PCR. *Biotechniques* **39**, 519–525 (2005).
50. Stern-Ginossar, N. *et al.* Host immune system gene targeting by a viral miRNA. *Science* **317**, 376–381 (2007).